The Danish Meteorological Institute

DMI Report 21-21 Arctic ocean and sea ice – from a Greenlandic fjord to large scale Arctic sea ice changes

Final scientific report of the 2020 National Centre for Climate Research Work Package 1.2.4, HavGRL

DMI Report
15 January 2021

By Till A. S. Rasmussen, Mads H. Ribergaard, Ida M. Ringgaard, Steffen M. Olsen, Andrea Gierisch and Vasily Korabel

The Danish Meteorological Institute

Colophon

Serial title	DMI Report
Title	DMI Report 21-21 Arctic ocean and sea ice – from a Greenlandic fjord to large scale Arctic sea ice changes
Subtitle	Final scientific report of the 2020 National Centre for Climate Research Work Package 1.2.4, HavGRL
Author(s)	Till A. S. Rasmussen, Mads H. Ribergaard, Ida M. Ringgaard, Steffen M. Olsen, Andrea Gierisch and Vasily Korabel
Other contributors	[Other contributors]
Responsible institution	Danish Meteorological Institute
Language	English
Keywords	Arctic sea ice, modelling, observations landfast sea ice,
URL	https://www.dmi.dk/publikationer/
Digital ISBN	978-87-7478-695-5
ISSN	2445-9127
Version	15 January 2021
Website	www.dmi.dk
Copyright	DMI

The Danish Meteorological Institute

Content

1 Abstract

The havGRL work package has three objectives. These are

1. Observations in Qaanaaq
2. High resolution hindcast 25 years back in time
3. Long time series of Arctic sea-ice and its feedback to the climate

The observations in Qaanaaq is a continuation of a unique observatory of a high latitude Arctic fjord, where DMI has conducted measurements of surface parameters as well as 3D oceanographic parameters. The equipment is installed, on the sea-ice when it becomes landfast, in late December and retrieved in May/June. The oceanographic measurements show that through time there has been a change in the water masses within the fjord, which could result in a change in the timing of the breakup of the land fast sea-ice and the opening of the North Water Polynya. These connections will be explored further in the upcoming NCKF. Thus, further investigations of the data is required. The surface measurements has proven to be valuable for validations of remotely sensed observations.

The second part of HavGRL focused on the continuous development of a high-resolution coupled ocean and sea-ice model. This includes many new features as for instance higher resolution, melt ponds, landfast sea-ice. All of these enables better near coastal hindcast and forecast, which is important as most people live and utilize these areas. A 25 year hindcast has been simulated and it has shown some promising results but also areas where further analysis are needed.

The focus of part three of this work package is on Arctic sea-ice and how feedbacks from major changes in the Arctic sea ice cover affects the future climate. This is achieved by analyses of five 30-year time slices from a 1350 year long (years 1850-3200) climate simulation following the RCP8.5 scenario. The five time slices represents 5 different states of the Arctic sea ice: 1) the pre-industrial state (1850-1879), 2) the present day state (1976-2005), 3) just after the Arctic becomes ice free in summer (2060-2079), 4) just after the arctic winter sea ice disappears (2154-2183) and by the end of the simulation, when the Arctic has been ice free for more than a thousand years (3170-3199). In the atmosphere, the loss of Arctic sea ice generally resulted in an equatorward shift of the ITCZ as well as intensified precipitation patterns. In the ocean, a warming and freshening of the Arctic Ocean was observed, as well a weakening of the Atlantic Meridional Overturning Circulation (AMOC).

2 Resumé

De to første dele af dette studie har fokus på forståelse af processer i havet og havisen og hvordan det giver en bedre forståelse af det nuværende klima. For at forstå hvad der sker i fremtiden er det nødvendigt at forstå det der sker nu. Den tredje del af studiet fokuserer på effekten af at havisdækket trækker sig tilbage og hvordan det påvirker atmosfæren og havet.

I det kystnære område er der fokuseret på en Grønlandsk fjord i nærheden af Qaanaaq i det nordvestlige Grønland. Det er vigtigt for lokalbefolkningen at vide hvornår isen ligger sig fast, da de er afhængige af at isen er stabil så de kan jage og transporterer sig på hundeslæde.
DMI har gennem en årrække haft en observations kampagne med base i Qaanaaq, hvilket NCKF er har fortsat. I oceanet er temperatur og saltholdighed blevet observeret. Formålet er at påvise om der er ændringer i de vandmasser der kommer sydfra langs den Grønlandske vestkyst. Samtidig er der målt overfladetemperature af is og sne og 2 meter lufttemperatur sammen med en række andre parametre. Derved kan man observere udviklingen af overfladeparametrene over en årrække. Samtidig giver det en unik mulighed for at validere telemåling resultater og at kalibrere disse observationer. Fordelen ved telemåling er at de kan give et globalt billede af vigtige klimaparametre som eksempelvis havisdækket og overfladetemperaturen af havis/sneen.
Observationskampagnen har sammen med analyser af tidligere in-situ observationer vist, at der er ændringer i vandmasserne i fjorden ved Qaanaaq, hvilket har betydning for den varme der er til rådighed for at smelte havisen og derved hvor lang fastis sæsonen er. Ændringen i fjorden gælder formodentlig andre steder langs den Grønlandske vestkyst. Eksempelvis Nordvandet, der er et område syd for Nares strædet og vest for Qaanaaq. Her åbner havisen normalt tidligere end de omkringliggende områder, hvilket giver anledning til stor biologisk produktion. Ændringer i timingen af åbningen af Nordvandet vil have indflydelse på dyrelivet i området.

På større skala har NCKF simuleret de sidste 20 års udvikling af havis og ocean cirkulation med en koblet ocean og havismodel. Formålet med dette er at få en forståelse af havisen både lokalt omkring Grønland og i Arktis. En af fokusområderne har været at undersøge om isbjerge har indflydelse på fastisen ved Grønland og om det kan implementeres i en havismodel, så det kan forudsiges. Dette dataarkiv kan i anvendes til at analysere trends af en række klimaparametre. Modelsimuleringerne har vist at det er muligt at modellere fastisen ved at tilføje indflydelse fra isbjerge. Samtidig har det gjort os i stand til at forudsige flere parametre som isens alder, smeltevandssøer og lignende.
Til sidst har en global klimamodel været anvendt til at analysere hvordan atmosfæren reagerer på at havisen trækker sig tilbage. Den lange klimatidsserie baseret på IPCC's scenario RCP 8.5 har vist at det Arktiske ocean bliver varmere og ferskere når isen forsvinder. Samtidig bliver AMOC (Atlantic Meridional Overturning Circulation) svagere. Derudover har det vist at atmosfærens cirkulation ændres helt ned til ækvator. Arbejdet vil resultere i en peer-reviewed artikel, der pt. går under arbejdstitlen "Climate change associated with sea ice loss in extended EC-Earth-PISM RCP8.5 simulation"

3 Introduction

The Danish National Centre for Climate Research (Nationalt Center for Klimaforskning, NCKF) has completed its first year in 2020. It has been a source of funding for the Danish Meteorological Institute and collaborators for climate change related research during this year. The 18 work packages fall under 4 general themes:
Arctic and Antarctic Research
Climate change in the near future
Use of climate data
Support for the IPCC

This work package havGRL is focused on the Arctic Ocean with special focus on the Greenlandic waters. Initially it was only focused on Greenlandic waters, however a merge of this and another work packages added an Arctic component to the work package. The work package now contains three main themes. These are

1. Observations in Qaanaaq
2. High resolution model of the future climate
3. Long time series of Arctic sea-ice and its feedback to the climate

This ranges from in-situ observations to modelling of high resolution features of the Arctic and Greenlandic waters and at last a long term climate simulation. The following three chapters will describe and motivate these

4 Qaanaaq observatory

Ocean variability and ocean-cryosphere interactions off NW Greenland from winter observations

A monitoring program of winter ocean and sea-ice conditions in the high-Arctic Inglefield Fjord was initiated by DMI in 2011 and continued in 2020 including a survey in spring and a winter climate observatory on ice. Observational data from this high Arctic fjord system form the basis to understand regional ocean variability and interactions with the cryosphere. Data are integrated into a line of research activities in Greenland Waters and interactions between ocean and cryosphere components. Here we briefly introduce the main features and list the publications in preparation.

The fjord is located in NW Greenland, open to the Baffin Bay at depths below 400m and typically covered by fast ice from December through June. In winter, an area of recurring open water, the North Water Polynya, reaches to the mouth of the fjord. This is maintained by prevailing northerly winds, ocean currents and partly facilitated by the formation of an ice-arch in the Nares Strait. A number of glaciers terminate into the fjord, the most prominent being Tracy and Heilprin. The town of Qaanaaq is located on the Northern coast in the outer part of the fjord.

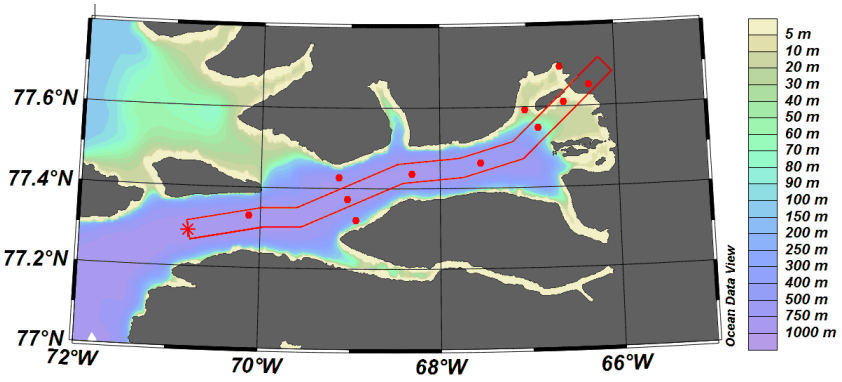

Figure 1 Map of Inglefield Fjord with typical hydrographic survey stations for the late winter campaign carried out in collaboration with local hunters. Red dots mark actual CTD sites.

Late-winter hydrographic surveys (Figure 1) and data from ice-tethered seasonal moorings document a persistent Atlantic warm core (AWC) at 300m depth throughout the length of the fjord. The most recent profile off Qaanaaq from December 2020 is shown in Figure 2 and reveals the main oceanographic features. This includes a typical cold winter mixed layer reaching here below 50m and a slightly eroded AWC were temperatures peak (300-350m) and a deep layer with decreasing oxygen content reflecting a gradual decline in ventilation intensity. Resuspension linked to the tidal currents explain the slightly elevated turbidity near the bottom in an otherwise featureless profile.

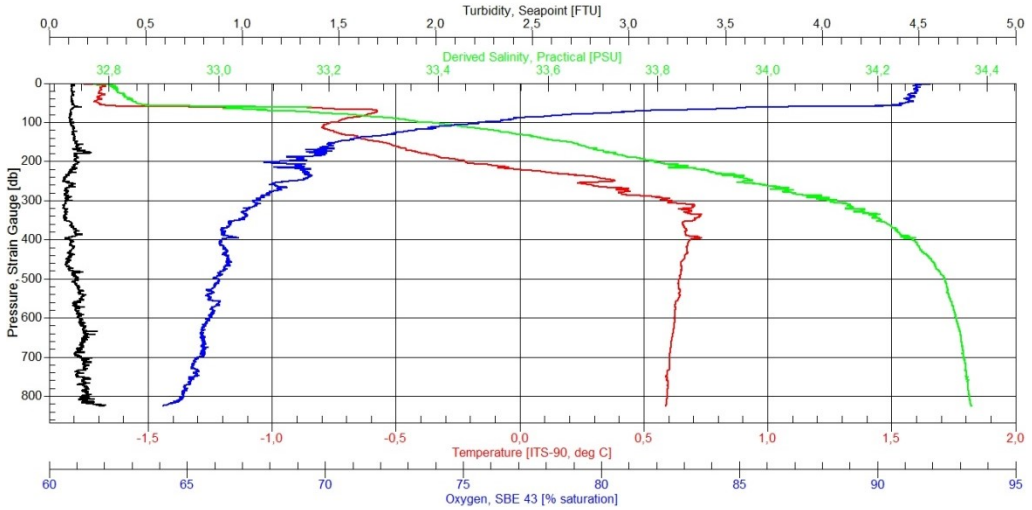

Figure 2 Full depth profiles of temperature (red), salinity (green), dissolved oxygen (blue) and turbidity (black) at station Q01 off Qaanaaq, Inglefield Bredning. 77 25.67 N, 69 08.07 W, 13 December 2020 19:00 UTC.

Interannual variability

From the dataset extending back to 2011, we find a signal of slow variability in the winter properties of the AWC with a peak in temperature in 2014 well above 1°C and a return to relatively low temperatures with 2020 not exceeding 1°C (Figure 2).
More striking is the interannual variability in upper stratification where two distinct modes are observed:

1) A locally formed brine enriched mixed-layer only 10-20m thick in the ice-covered part of the fjord.

2) A roughly 100m deep mixed-layer with characteristics of the off-shore North Water Polynya extends throughout the length of the fjord.

These modes affect the formation and growth rate of fast ice and are the primary cause for variations in the melt potential of marine terminating glaciers.
Above the AWC, modified waters result from latent cooling from ice melt and subsequent mixing with the melt water. In addition, a lens of water resting below the mixed layer shows evidence of mixing with a liquid freshwater source, possibly subglacial discharge. We explain the different configurations of the upper stratification accordingly: In years where the Polynya water is anomalously light, modified Atlantic water by glacier interaction is not sufficiently buoyant to destabilize this stratification and Polynya water then occupies the entire fjord. The main driver of the changes in the fjord is found to be the conditions in the Polynya. Here we observe a pronounced densification and salinification until 2017/2018 of the winter mixed-layer.

Results and data are planned to be presented in following publications:[Munchow, 2021], [Ribeiro S, 2021] and

5 High resolution Arctic and Greenlandic model

A new high resolution ocean and sea ice model has been implemented. The components of the model system are HYCOM (ocean) [Metzger et al, 2014], CICE [Hunke et al, 2020] and ESMF(coupler) [Hill et al, 2014]. The system covers the area from 20° south and includes the North Atlantic and the Arctic ocean. The bathymetry of the domain is shown in Figure 3. The resolution is ~5km in the Arctic and the Greenlandic waters.

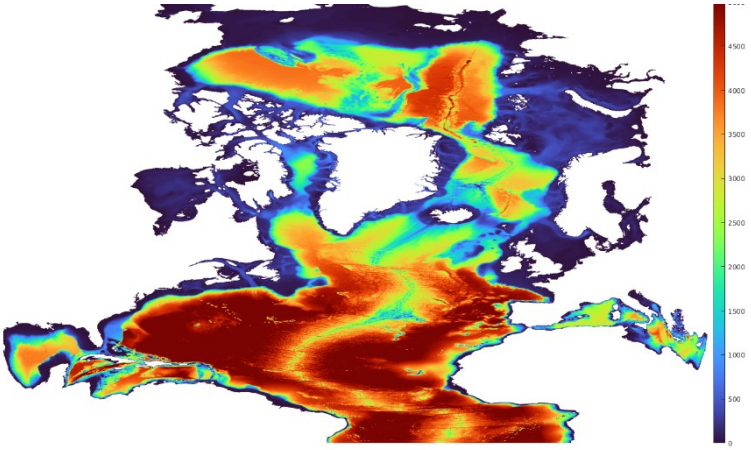

Figure 3 Bathymetry of model domain

A 25 year hindcast has been simulated with the model system. This upper boundary has been determined by ERA-5. Studies has shown that this atmospheric reanalysis is generally to warm in Arctic, see for instance [Wang, 2019]. This results in a sea ice cover that in general is too small. In order to fix this issue a reduction by 10% of the incoming short wave radiation was introduced. The reduction is only applied in Arctic, where there is sea-ice. The effect of this in winter is limited, however it does result in a better summer ice cover.

An example of this is shown in Figure 4

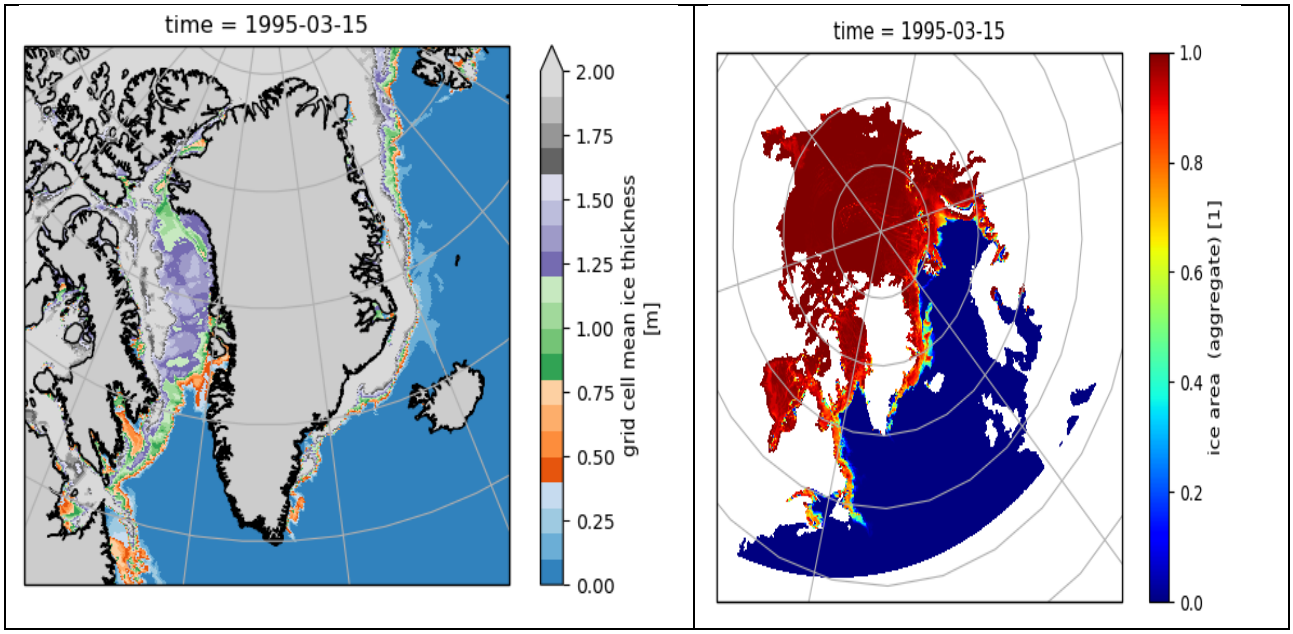

Figure 4 Snapshots of ice thickness around Greenland to the left and Arctic ice concentration to the right.

The two figures show a reasonable ice cover (right) and ice thickness (left), however further analysis of the system should be carried out in order to validate ad analyse trends etc.

Compared to previous simulations it includes a range of new physical properties that are proxies of the climate and the change in the climate over the last 25 years. With the increased resolution and the new features, it allows us to analyse several proxies for the changing climate. Some of these are shown in Table 1.

Ice age	Ice age is an indicator of thick sea ice and it is often used by
Prognostic salinity	Important for instance conductivity.
Advanced albedo schemes	Improved heat uptake
Form drag	Sea ice has traditionally be
Landfast sea ice	This is important for where leads open. Without landfast sea ice lead often open near the coast. With this

Table 1 New sea ice parameters in CICE 6

5.1 Landfast sea-ice

Landfast sea-ice is sea-ice that remains immobile for a period of time. This is of great importance for the locals in Greenland as the they use it to hunt from and travels across the fjords.

An example of the landfast sea-ice is shown in Figure 5

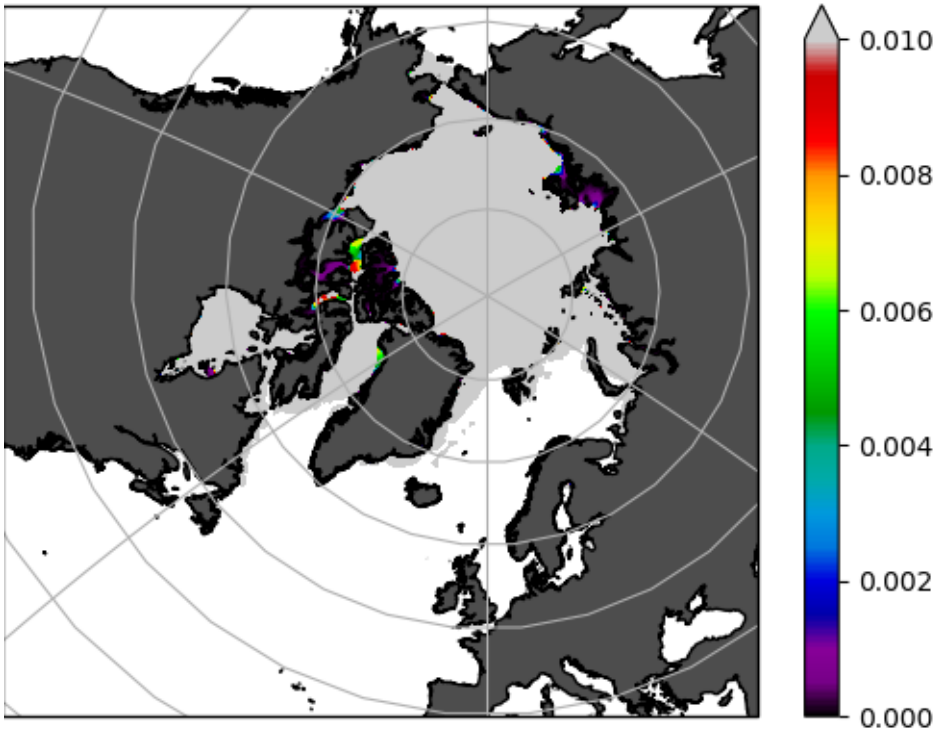

Figure 5 Landfast sea-ice March 1995. Categorized to be landfast when velocity is lower than 0.01 m/s. The ice cover is shown for ice concentrations higher than 85%

Landfast sea ice is here defined to be present when average sea-ice velocities are less than 0.01 m/s. With this definition Figure 5 show that the model predicts landfast ice near the Siberian coast, in the Canadian Archipelago and a bit near the Greenlandic coast. This matches observations reasonably well; however, there are places near the Greenlandic coast, where landfast sea-ice is missing.
The new model setup do have implementations of landfast sea-ice, however this is based on shallow water where ridges reach the seabed and sea-ice is locked to islands This is rarely the case around Greenland where waters are often too deep. This study test a hypothesis that icebergs ground, and then sea-ice grows around it and stop the sea-ice drift. First step is to investigate the mobility of the icebergs.

This is shown in Figure 6

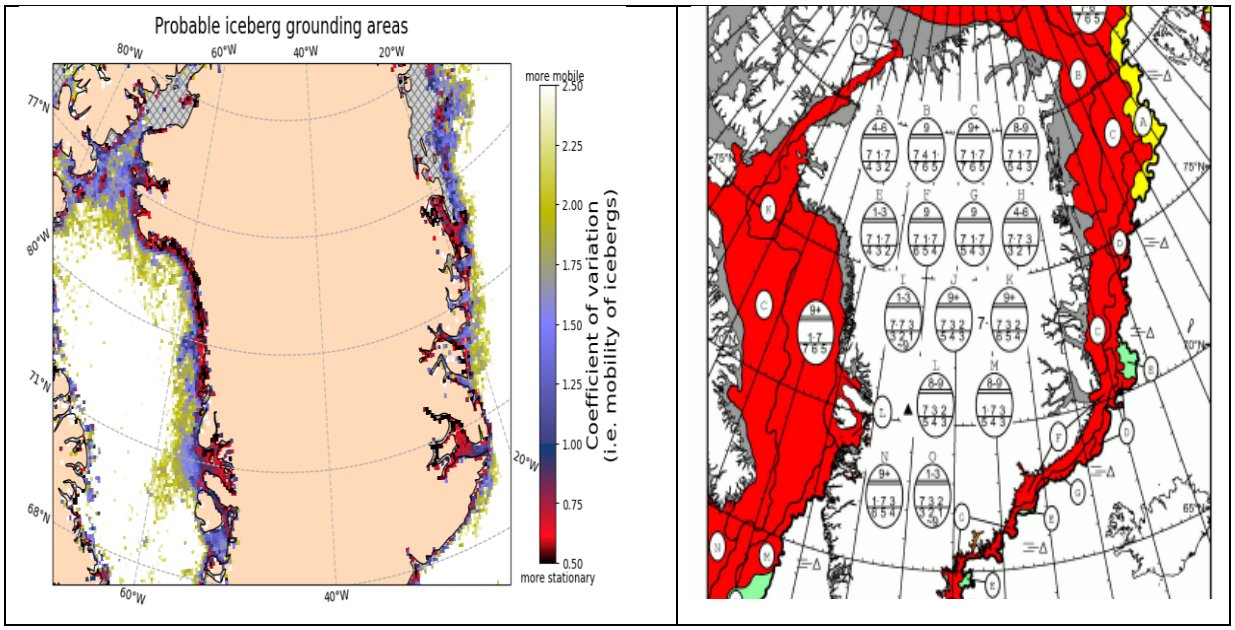

Figure 6 Left figure: Probability of stationary ice bergs. Right figure gray areas show grounding zones based on ice charts

In order to compare the likely grounding zones a comparison with ice charts and their landfast ice zones is made. The iceberg mobility zone is shown to the left and to the right as gray areas in the icehart .The grounded icebergs show a reasonable correlation with the landfast sea-ice based on icecharts. In order to model the landfast sea-ice a friction term has been added to the momentum equation for sea ice. The friction is a function of the mobility of the icebergs (CoV).

$$\tau_b = f(CoV) = \frac{2}{e^{CoV^{1.5}-0.59}} \qquad (1)$$

The result of a reference run and a run with equation 1 added is shown in Figure 7.

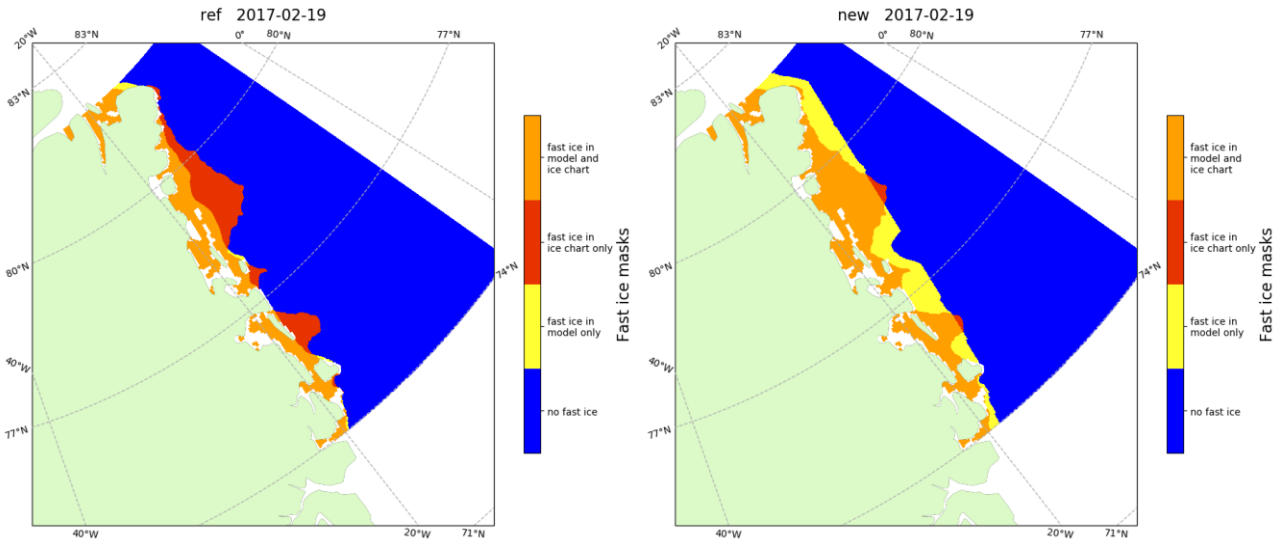

Figure 7 Example of simulation with and without the iceberg grounding implementation. Left reference run without implementation of icebergs. Right same simulation with iceberg grounding implemented. Blue indicates areas without fastice, yellow indicates areas with fast ice, red only landfast ice in the observation (icecharts) and orange landfast ice both in model simulation and observation.

It is clear that the landfast ice parameterization outlined in equation 1 results in more landfast ice at the approximate correct location, thus the results are promising. That being said the constants in equation 1 might need a bit of tuning in order to improve the results even further.

6 Global simulation – Climate change associated with sea ice loss

The ongoing decline of the Arctic sea ice is expected to continue in the future. Potential implications on climate due to the transition from a perennial Arctic sea ice cover, to a seasonal ice cover and finally to an ice-free Arctic Ocean is investigated using a 1350 year (years 1850-3200) long RCP8.5 scenario simulation. This simulation uses the model EC-Earth-PISM: This is an atmosphere-ocean general circulation model coupled to an interactive Greenland Ice Sheet model through the ice sheet model PISM. Five 30-year time periods were compared: the pre-industrial period (P1), the present day period (P2), the period just after the Arctic summer sea ice disappeared (P3), the period just after the Arctic winter sea ice disappeared (P4) and the end of the simulation when the Greenland ice sheet have shrunk by 62% (P5), see Figure 8. In this simulation, the Arctic sea ice is projected to disappear in September in year 2060 and in March by year 2154.

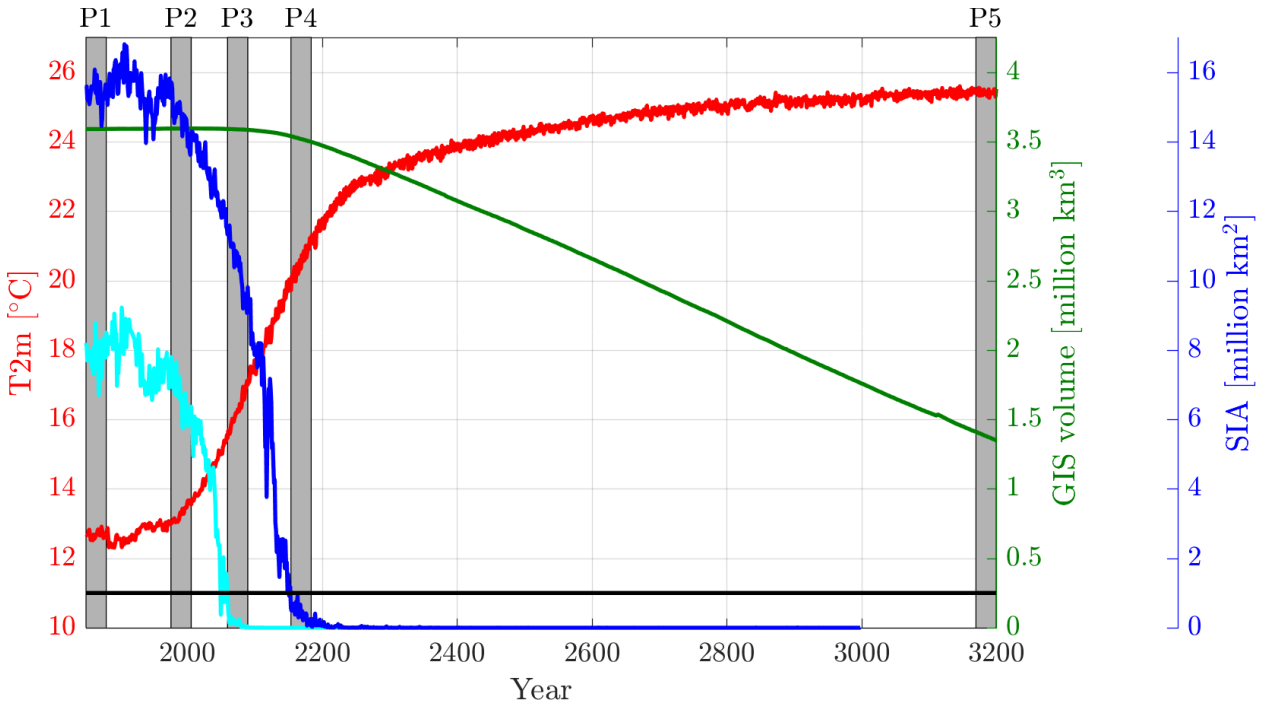

Figure 8: Annual global mean surface (2m) air temperature (red; in °C), annual Greenland Ice Sheet Volume (green; in million km^3) and mean Northern Hemisphere Sea ice area (in million km^2) for March (dark blue) and September (light blue) in the EC-Earth-PISM RCP8.5 simulation. Horizontal line indicate SIA equal to one million km^2. The 5 grey boxes indicate the 5 periods defined in table 1. The temperature for year 2571 has been removed, as there was a spurious spike in temperature for this year. The spike occurred due to an error in the forcing setup.

The Arctic Amplification is projected to peak around P2 and P3, gradually weakening afterward, but not disappearing, by P5 (Figure 9). Hence, the Pole-Equator temperature gradient decreased as the Arctic sea ice disappeared.

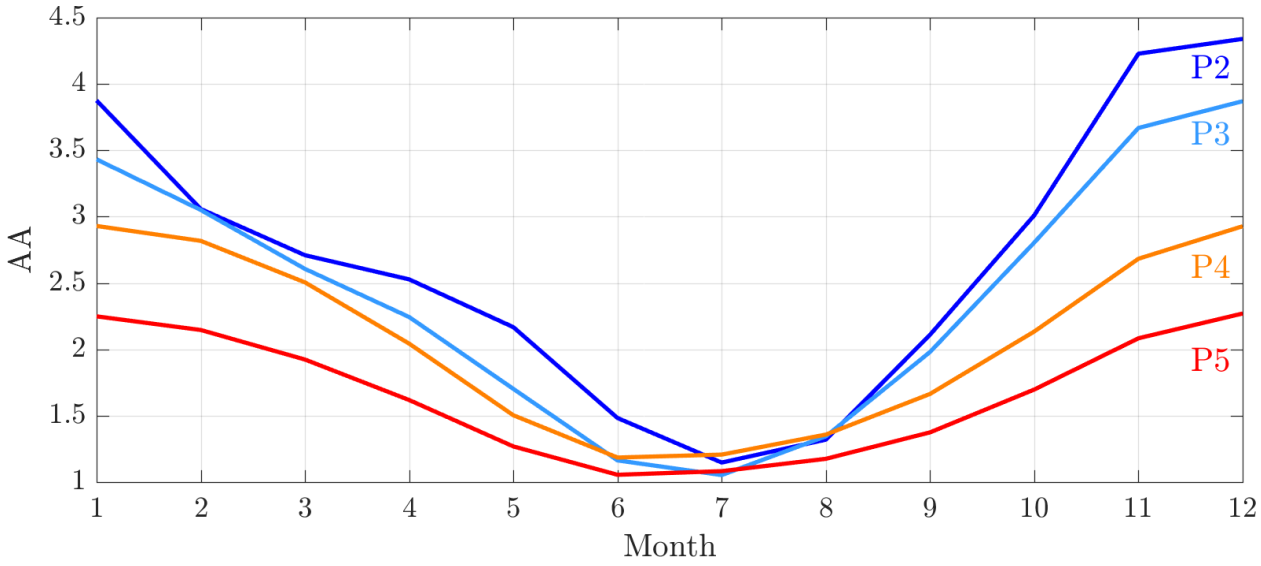

Figure 9: Arctic amplification, relative to P1 (1850-1879) for P2 (dark blue), P3 (light blue), P4 (orange) and P5 (red).

The atmospheric circulation showed an equatorward shift, as illustrated by the stream function in Figure 10.

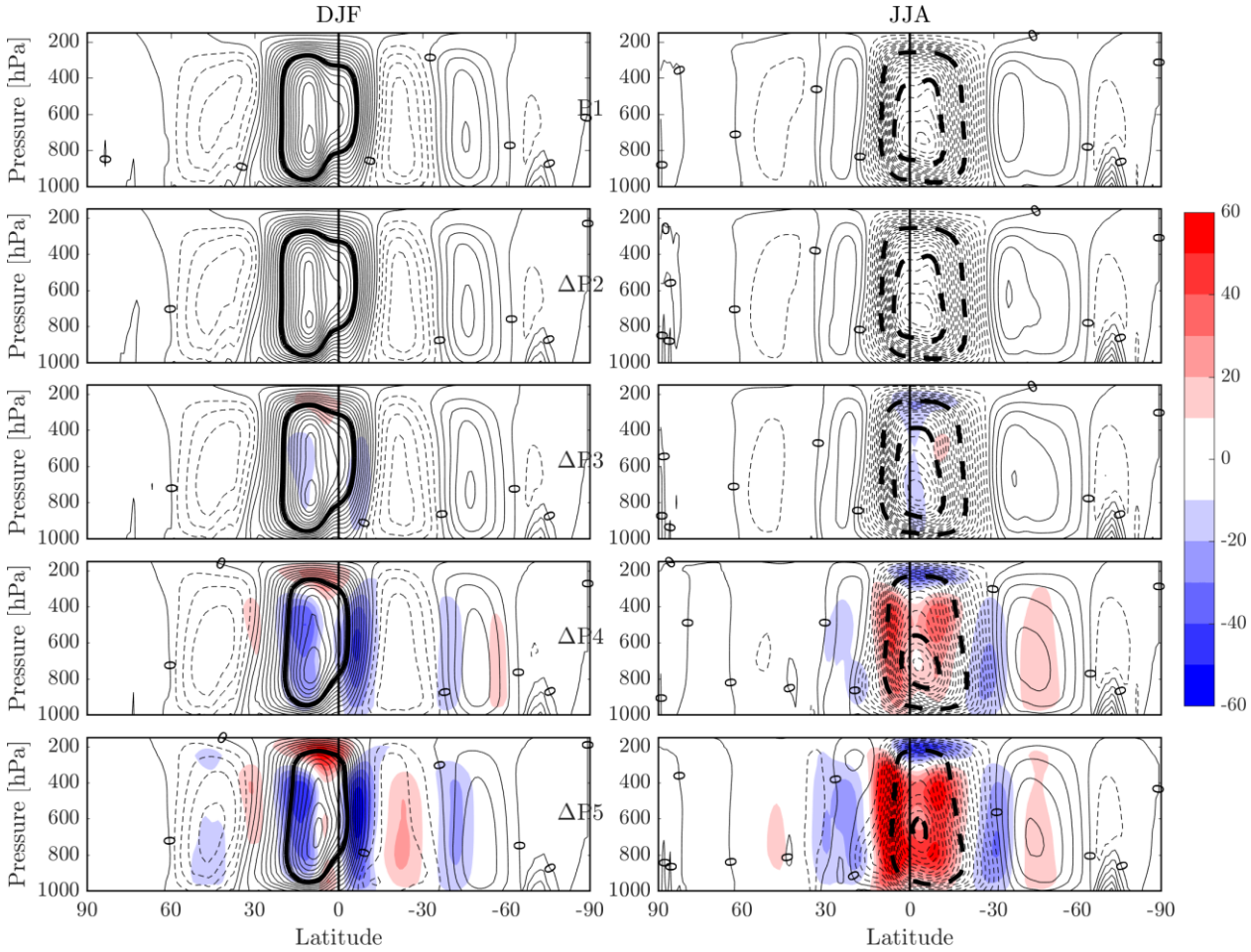

Figure 10: Stream function (in 10^9 kg s^{-1}) for P1 (top row) for DJF (left column) and JJA (right column). The four rows below show the stream functions for P2 to P5 (contours) and the difference relative to P1 (shading; in 10^9 kg s^{-1}) The interval for the thin contour lines is $10x10^9$ kg s^{-1} and $100x10^9$ kg s^{-1} for the thick contour lines. Positive is counterclockwise flow (solid lines + red shading) and negative is clockwise flow (dashed lines + blue shading).

The ocean changes were similar to those found by Koenigk et al. (2016): a warmer and fresher Arctic Ocean and increased heat transport into the Arctic Ocean through the Barents Sea. The freshening of the Arctic Ocean was most likely due to increased precipitation, not Greenland ice sheet melt. Further, a weakening of the AMOC is observed (Figure 11). The rate of change of these oceanic parameters was largest around P3 and P4, similar to the atmospheric changes. The ocean circulation stabilized after P4, while the temperature and salinity in the Arctic Ocean continued to increase and decrease, respectively.

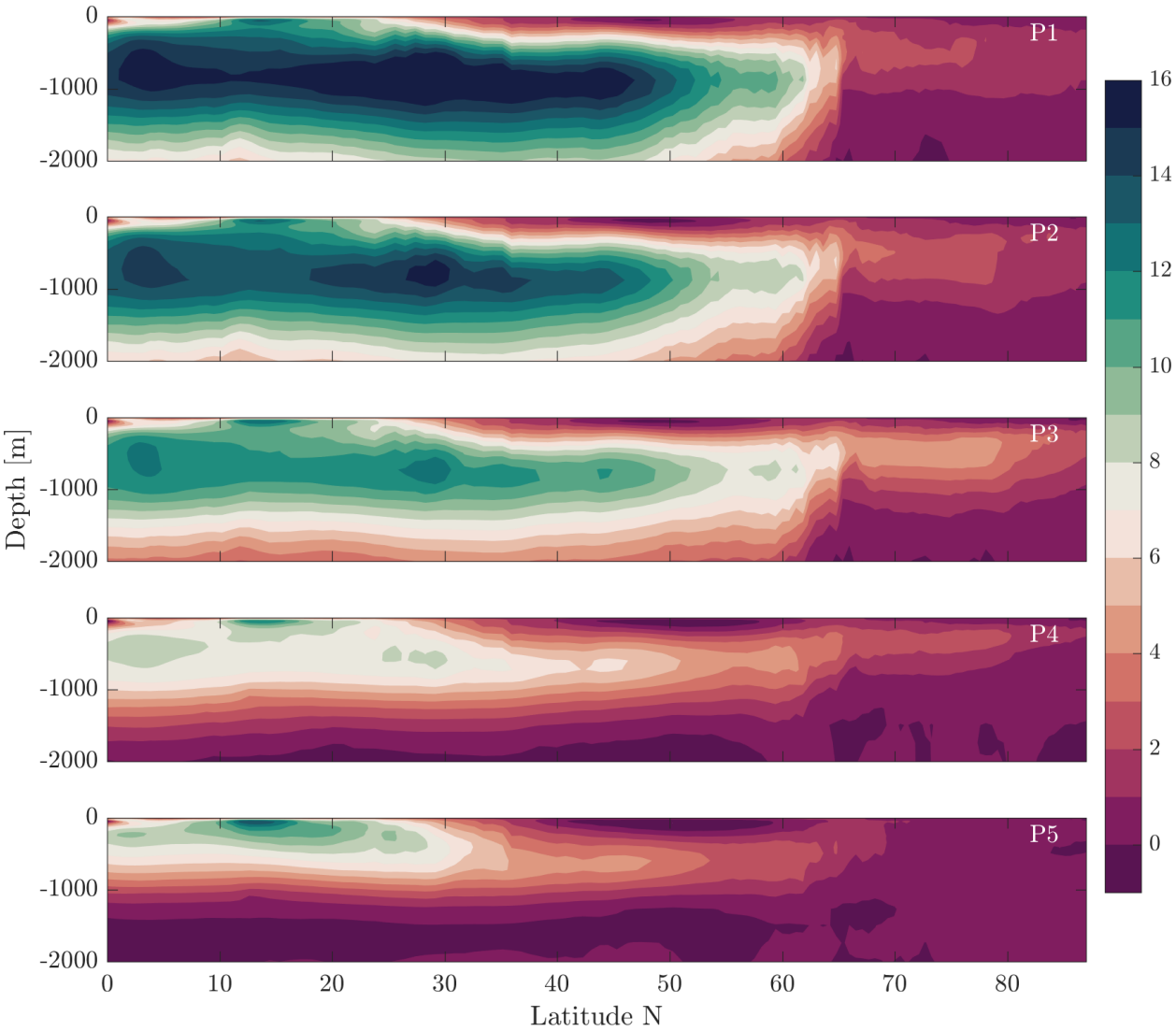

Figure 11: 30-year mean of the AMOC (in Sv) for each time period.

Our preliminary results indicate that the sea ice state might affect the rate of some climatic changes. However, the rapid sea ice decline coincides with a rapid increase in global mean temperature and anthropogenic GHG emissions. Separating the influence of the sea ice loss, the increasing temperature and GHG emissions require further analysis. Additional analysis could be to investigate the impacts on Greenland more closely.

Further details can be found in [Ringgaard et al., 2021];

7 NCKF related publications

In total 7 publications with relations to this work package has been accepted, submitted or drafted. These are

- [Hunke et al, 2020] (published)
- [Hutter et al, 2021], (in preparation)
- [Bouchat et al, 2021] (in preparation)
- [Jackson et al, 2021] (submitted)
- [Munchow et al, 2021] (in preparation)
- Ribero et al, 2021] (submitted)
- [Ringgaard et al, 2021] (in preparation)

8 References

Bouchat A., Hutter N., Dupont F., Dukhovskoy D, Garric G, Lee Y, Lemiux J. F., Lique C. Losch M., Maslowski M, Myers P. Olson E., Rampal P., **Rasmussen T.** , Talandier, Tremblay B. Wang Q.; Sea Ice Rheology Experiment (SIREX), Part 1: Scaling and statistical properties of sea-ice deformation fields. (in preparation, 2021)

Hill, C.; Deluca, C.; Balaji; Suarez, M.; Da Silva, A. (2004). "The architecture of the earth system modeling framework". Computing in Science & Engineering. 6 (1): 18–28. Bibcode:2004CSE.....6a..18H. doi:10.1109/MCISE.2004.1255817. S2CID 9311752. Hunke et al; CICE model; 10.5281/zenodo1205674

Hutter N., Bouchat A, Chanut J,, Dupont F., Dukhovskoy D, Koldunov N., Lee Y., Lique C. Losch M., Maslowski M, Myers P. Olson E., Rampal P., **Rasmussen T.** , Talandier, Tremblay B., Wang Q.; Leads and pressure ridges simulated by high-resolution sea-ice models within the FAMOS sea ice rheology experiments (SIREx (in preparation, 2021)

*2021 Jackson, R., Kvorning, A. B., Limoges, A., Georgiadis, E., **Olsen, S.M**., Tallberg, P., Andersen, T.J., Mikkelsen, N., Giraudeau, J., Massé, G., Wacker, L. and S. Ribeiro. Holocene polynya dynamics mediate ocean heat transport in northern Baffin Bay (submitted)

Koenigk T. , M. Calan, G. Nikulin, and S. Schimanke Regional Arctic Sea ice variations as predictor for winter climate conditions. Climate Dynamics; 46:317–337, 2016.
Metzger et al. US Navy operational global ocean and Arctic ice prediction system. Oceanography 27(3):32-43, http://dx.doi.org/10.5670/oceanog.2014.66
*Climate change associated with sea ice loss in extended EC-Earth-PISM RCP8.5 simulation; to be submitted
Metzger, E.J., O.M. Smedstad, P.G. Thoppil, H.E. Hurlburt, J.A. Cummings, A.J. Wallcraft, L. Zamudio, D.S. Franklin, P.G. Posey, M.W. Phelps, P.J. Hogan, F.L. Bub, and C.J. DeHaan. 2014. US Navy operational global ocean and Arctic ice prediction systems. Oceanography 27(3):32–43, http://dx.doi.org/10.5670/oceanog.2014.66.
*2021 Muenchow, A. and **S.M. Olsen**. Decadal ocean variability off North Greenland and its atmospheric forcing (in prep).
*2021 Ribeiro S., Limoges, A., Massé, G., Johannsen K. L., Colgan, W., Weckström, K., Jackson, R., Georgiadis, E., Mikkelsen, N., Kuijpers, A. Olsen, J., **Olsen, S.M**., Nissen, M., Strunk, A., Wetterich, S., Syväranta, J., Henderson, A.C.G., Mackay, H., Taipale, S., Jeppesen, E., Larsen, N.K., Crosta, X., Giraudeau, J., Nuttall, M., Holm, L.K., Grønnow, B., Mosbech, A. and T.A. Davidson. Vulnerability of the North Water polynya ecosystem to climate change (submitted)
Ringgard I. M, Yang S., Kaas E, Christensen J.; 2021Climate change associated with sea ice loss in extended EC-Earth-PISM RCP8.5 simulation

Wang, C., Graham, R. M., Wang, K., Gerland, S., and Granskog, M. A.: Comparison of ERA5 and ERA-Interim near-surface air temperature, snowfall and precipitation over Arctic sea ice: effects on sea ice thermodynamics and evolution, The Cryosphere, 13, 1661–1679, https://doi.org/10.5194/tc-13-1661-2019, 2019.

9 Previous reports

Previous reports from the Danish Meteorological Institute can be found on:
https://www.dmi.dk/publikationer/